Correlation-based detection of TCM signals for Cognitive Radios

Reza Soosahabi[1], Mort Naraghi-Pour[2], Nasim Nasirian[3], Magdy Bayoumi[3]
[1]Distributed Computing & Communications Lab, Infolink-USA Inc., Lafayette, LA70508
[2]Division of Electrical & Computer Engineering, Louisiana State University, Baton Rouge, LA70803
[3]The Center for Advanced Computer Studies, The University of Louisiana, Lafayette, LA70503
emails: rsoosahabi@infolink-usa.com, naraghi@lsu.edu, nxn5303@louisiana.edu, mab@cacs.louisiana.edu

***Abstract*—In this work, the inter-dependency of TCM signals is studied. Using this inter-dependency, correlation-based detectors are proposed for spectrum sensing of TCM signals in white Gaussian noise. In particular, a constant false alarm rate (CFAR) detector is presented and its performance is evaluated using simulations. We also describe an application of our detector for the classification of uncoded modulation systems vs. their TCM counterparts and present numerical results on their performance.**

***Index Terms*—Spectrum Sensing, Cognitive Radio, Trellis Coded Modulation, Correlation, Signal Detection**

I. Introduction

Opportunistic spectrum access (OSA) has been proposed for alleviating the overcrowding of the radio spectrum [1], [2]. Spectrum sensing is a key function in OSA which allows a cognitive radio (CR) to identify and utilize an unused licensed spectrum without undue interference to the primary users [3]. After detecting the spectral white space a frequency agile CR can adjust its transmitter parameters including its frequency, modulation, coding, power, etc., in order to make best use of the available spectrum. Several techniques have been proposed for spectrum sensing in recent years [4]–[7], including energy detectors, [8], [9], cyclostationary detectors, [10], [11], and autocorrelation-based detectors, [12]–[14].

Correlation-based techniques are commonly used in various areas of wireless communication. In spectrum sensing, correlation-based detectors can be designed to have the CFAR (constant false alarm rate) property [14]–[16]. For such detectors the false alarm probability does not depend on the noise power. Therefore a Neyman Pearson type detection method can be easily implemented whereby the decision threshold is simply computed from the desired value of false alarm probability.

Trellis coded modulation (TCM) is a popular scheme for information transmission over bandlimited channels which achieves good power and bandwidth efficiency [17]. Since its inception, TCM has been one of the most active areas of research in communications and has been proposed for many wired and wireless communication systems, [18], [19], including video and TV broadcasting [20], [21]. A recent application of TCM involves millimeter-wave radio links that provide Gigabit wireless back-haul to the small-cells in the new generation of cellular networks (5G). [22], [23].

Our goal in this paper is to develop a correlation-based detector for TCM-type signals. Towards this end we first investigate the inter-dependency properties of TCM symbols. It is clear that the presence of a trellis structure imposes such an inter-dependency among TCM symbols. However, it is shown that, for most TCM structures of interest, an autocorrelation-based detector will not be effective due to the fact that, surprisingly, any two symbols from the TCM code are independent. However, it is shown that $\nu+1$ consecutive symbols, where ν is the code's constraint length, are dependent. Using this property we introduce three different decision statistics which are derived from one another with improved properties. The third scheme for which we present simulation results is a CFAR detector. We also describe an application of our approach for the classification of an uncoded modulation scheme vs its TCM counterpart.

In Section II we study the correlation properties of TCM signals. In Section III we describe our decision statistics for spectrum sensing of 8-PSK TCM schemes. Section IV describes the application of our approach to modulation classification. Numerical results are presented in Section V and conclusions are drawn in Section VI.

II. Correlation Properties of TCM Signals

Trellis coded modulation (TCM) is a combined coding and modulation technique suitable for transmission over bandlimited channels. The main attraction of TCM stems from the fact that it achieves significant gains in SNR over the uncoded systems without the concomitant bandwidth expansion of traditional coded modulation systems [17]. A block diagram of a TCM encoder is shown in Fig. 1. From the set of m information bits, $\bar{m}$ bits are encoded using a rate $\frac{\bar{m}}{\bar{m}+1}$ convolutional code with constraint length ν. The $\bar{m}+1$ bits are then used to select a subset (containing $2^{m-\bar{m}}$ signals) of a redundant $M=2^{m+1}$-ary signal set $\mathcal{S}=\{\mathbf{s}_0,\mathbf{s}_1,\cdots,\mathbf{s}_{M-1}\}$. The remaining $m-\bar{m}$ uncoded bits are used to select a signal from the subset for transmission. The selection of the subsets is performed by *set partitioning* which increases the minimum Euclidean distance of the signals in the subset with each partition [17]. The convolutional encoder imposes a trellis structure on the sequence of transmitted symbols which describes the dependency of a transmitted symbol on previously transmitted symbols. This dependency is used to increase the Euclidean distance between distinct sequences of symbols corresponding to distinct code paths. An example for the 8-PSK signal constellation is shown in Fig. 2 [24].

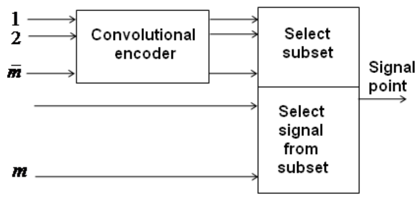

Fig. 1: Block diagram of the TCM encoder.

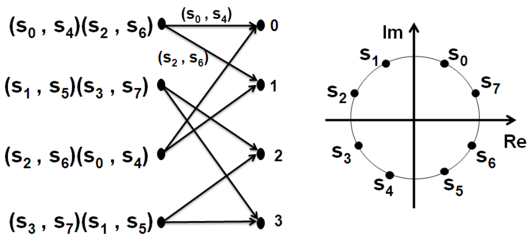

Fig. 2: TCM trellis ($\nu = 2$) and 8-PSK signal constellation.

In this paper we are interested in the inter-dependency of the transmitted symbols in a TCM system. At the first glance it may appear that each pair of consecutive symbols are dependent. This, however, is not true for most trellises of interest. In particular, let $\{X_n\}$ denote the sequence of symbols from the signal constellation which represents a coded path in the trellis with X_n denoting the (output) symbol at time n. Also let $\{S_n\}$ denote the sequence of states of the trellis with S_n denoting the state at time n. Then any $\nu + 1$ consecutive symbols $X_{n-\nu+1}, X_{n-\nu+2}, \cdots, X_{n+1}$ are dependent. This is due to the fact that, regardless of what the state at time $n-\nu$ is, the symbols $X_{n-\nu+1}, X_{n-\nu+2}, \cdots, X_n$ uniquely identify the state S_n at time n. Now since only 2^m branches emanate from this state, it follows that

$$P(X_{n+1} = \mathbf{s}_j | X_{n-\nu+1} = \mathbf{s}_{k_{n-\nu+1}}, \cdots, X_n = \mathbf{s}_{k_n}) = \frac{1}{2^{m-\bar{m}}} \quad (1)$$

where we have assumed that the signals in the constellation are used with equal frequency [17]. On the other hand, $P(X_{n+1} = \mathbf{s}_j) = \frac{1}{2^{m+1}}$. This and (1) imply that the symbols $X_{n-\nu+1}, X_{n-\nu+2}, \cdots, x_n, X_{n+1}$ are dependent. Note that this property is independent of the signal constellation or the rule which maps the symbols to the branches of the trellis as long as in every stage of the trellis the signals are used with equal frequency [17].

An important question is whether fewer than $\nu + 1$ output symbols can be dependent. In fact some TCM structures have the property that $k < \nu + 1$ output symbols are dependent. For example consider the trellis of Fig. 2. At each stage the trellis contains 16 branches. Therefore if this trellis is used with a 16-PSK modulation scheme, then each output symbol uniquely identifies the next state. Therefore any two consecutive symbols will be dependent. Such TCM structures, however, do not have good distance properties and will not be considered further in this paper.

For the trellis in Figs. 2 with 8-ary PSK, any set of fewer than $\nu + 1$ symbols are independent such that for any $\ell \geq 0$,

$$P(X_{n+1} = \mathbf{s}_j | X_{n-\ell} = \mathbf{s}_i) = P(X_{n+1} = \mathbf{s}_j), \ \forall \ i, j. \quad (2)$$

In other words, any two (consecutive) symbols in a coded sequence are independent. This implies that $R_{XX}(k) = E[X_{n+k}X_n^*] = 0$ for $k \neq 0$. Therefore, for this TCM structure, autocorrelation-based spectrum sensing techniques will be ineffective for detecting the presence or absence of TCM signals in white Gaussian noise. For that purpose at least three consecutive symbols must be considered.

Although our results can be easily generalized for arbitrary TCM structures, for concreteness and ease of notation, in the remainder of this paper we confine our attention to the 8-PSK TCM scheme of Fig 2.

III. Spectrum Sensing for 8-PSK TCM

Based on the observation in the previous section a test statistic can be formed for detection of TCM signals in white Gaussian noise. Consider the signal $r(t)$ received by a secondary user in a CR network, where $r(t) = \eta s(t) + v(t)$, and where $\eta = 1$ and 0 indicates the presence or absence of the primary user signal, respectively. We assume that the signal $s(t)$ is an 8-PSK TCM signal. After down conversion and sampling the received signal samples are given by $\mathbf{r}_n = \eta x_n + v_n$, where $x_n \in \mathcal{S}$ and v_n is a complex circular Gaussian random variable with mean zero and variance $2\sigma^2$.

We denote the case of $\eta = i$ with the hypothesis $\mathcal{H}_i$, $i = 0, 1$. Our goal is to devise a simple decision statistic based on the received sequence $\mathbf{r} = (\mathbf{r}_0, \mathbf{r}_1, \cdots, \mathbf{r}_{N-1})$ that can be used to detect the hypothesis $\mathcal{H}_\eta$.

A. A binary decision statistic

For the 8-PSK TCM of Fig. 2 we define the following mappings.

$$q(x) = \begin{cases} +1 & \text{if} \quad x \in \{\mathbf{s}_0, \mathbf{s}_4, \mathbf{s}_3, \mathbf{s}_7\} \\ -1 & \text{if} \quad x \in \{\mathbf{s}_1, \mathbf{s}_2, \mathbf{s}_5, \mathbf{s}_6\} \end{cases} \quad (3)$$

$$Q(x) = \begin{cases} +1 & \text{if} \quad x \in \{\mathbf{s}_0, \mathbf{s}_2, \mathbf{s}_4, \mathbf{s}_6\} \\ -1 & \text{if} \quad x \in \{\mathbf{s}_1, \mathbf{s}_3, \mathbf{s}_5, \mathbf{s}_7\} \end{cases} \quad (4)$$

Then it can be verified that for any sequence of coded symbols $\{x_n\}$ the following holds for any time n.

$$q(x_{n-2})\ Q(x_{n-1}) = q(x_n) \quad (5)$$

To develop a test statistic using (5), we extend the mappings q and Q to the entire complex plane as depicted in Fig. 3. We now define the following test statistic using the binary functions $q^e(\cdot)$ and $Q^e(\cdot)$.

$$T_1(\mathbf{r}) = \frac{1}{N-2} \sum_{n=2}^{N} t_n \quad (6)$$

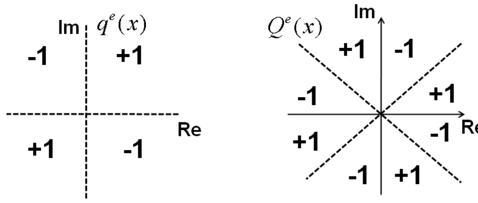

Fig. 3: Extensions of the mappings q and Q.

where $t_n = q^e(\mathbf{r}_{n-2})Q^e(\mathbf{r}_{n-1})q^e(\mathbf{r}_n)$. Our motivation for (6) is that since the noise is circularly symmetric, in the absence of the primary signal $E(t_n|\mathcal{H}_0) = 0$ which implies that $E[T_1(\mathbf{r})|\mathcal{H}_0] = 0$. On the other hand, due to (5), $E(t_n|\mathcal{H}_1) = \rho > 0$ implying that $E[T_1(\mathbf{r})|\mathcal{H}_1] = \rho > 0$, where ρ depends on the SNR. Although $T_1(\mathbf{r})$ can be used for the detection problem at hand, since the value of ρ is small, its performance under low SNR regime is poor. The difficulty is due to the hard quantization effect of the mappings $q^e(\cdot)$ and $Q^e(\cdot)$. To resolve this problem we introduce a new mapping in the following.

B. A hyperbolic mapping

Consider the two mappings $a(z) = xy$ and $b(z) = xy(x^2 - y^2)$ defined on the complex plane where $x = \Re(z)$ and $y = \Im(z)$. A new decision statistic is defined by

$$T_2(\mathbf{r}) = \frac{1}{N-2}\sum_{n=2}^{N}\tau_n \tag{7}$$

where $\tau_n = a(\mathbf{r}_{n-2})b(\mathbf{r}_{n-1})a(\mathbf{r}_n)$.

Remark: We would like to note the similarity between t_n and τ_n. In particular, in the absence of noise, we have $t_n = 1$ and $\tau_n = E^4$, where E is the energy of the 8-PSK signals.

It is straightforward to show that $E[T_2(\mathbf{r})|\mathcal{H}_0] = 0$ and $\mathrm{var}[T_2(\mathbf{r})|\mathcal{H}_0] = \frac{4\sigma^{16}}{N-2}$. Now by the central limit theorem on weakly dependent sequences, $\sqrt{N-2}\ T_2(\mathbf{r}) \sim \mathcal{N}(0, 4\sigma^{16})$. Therefore, for large N, the probability of false alarm is approximated by

$$P_F = P(T_2(\mathbf{r}) > \lambda|\mathcal{H}_0) = Q\left(\frac{\lambda\sqrt{N-2}}{2\sigma^8}\right). \tag{8}$$

It can also be shown that $E[T_2(\mathbf{r})|\mathcal{H}_1] = E^4/16$. The variance of the decision statistic under $\mathcal{H}_1$ is more difficult to compute. Therefore it is difficult to obtain a closed from solution for the detection probability. However, this variance goes to zero with N and so $P_D \longrightarrow 1$ with N. In the following we present a third decision statistic which improves upon $T_2(\mathbf{r})$.

C. A CFAR decision statistic

Two new mappings $\alpha(z)$ and $\beta(z)$ are defined on the complex plane as follows. For $z = x + jy = |z|e^{j\theta}$, let $\alpha(z) = \frac{2xy}{|z|^2} = \sin(2\theta)$ and $\beta(z) = \frac{4xy(x^2-y^2)}{|z|^4} = \sin(4\theta)$. The new decision statistic is now defined by

$$T_3(\mathbf{r}) = \frac{1}{N-2}\ \sum_{n=2}^{N}\chi_n \tag{9}$$

where

$$\begin{aligned}\chi_n &= \alpha(\mathbf{r}_{n-2})\beta(\mathbf{r}_{n-1})\alpha(\mathbf{r}_n) &(10)\\ &= \sin(2\theta_{n-2})\ \sin(4\theta_{n-1})\ \sin(2\theta_n) &(11)\end{aligned}$$

and where $\theta_i = \arg \mathbf{r}_i$. An important feature of this detection statistic is that it is a constant false alarm rate (CFAR) detector. This implies that for a given probability of false alarm, P_F, we can compute the appropriate threshold to implement the detector. The following results can be easily verified.

$$\begin{aligned}E(T_3(\mathbf{r})\,|\mathcal{H}_0\,) &= 0 &(12)\\ Var(T_3(\mathbf{r})\,|\mathcal{H}_0) &= \frac{1}{8(N-2)} &(13)\end{aligned}$$

$$P_F = P(T_3(\mathbf{r}) > \lambda \mid \mathcal{H}_0) = Q(\sqrt{8(N-2)}\lambda) \tag{14}$$

For a given value of P_F, the threshold λ can be evaluated from (14) as $\lambda = Q^{-1}\left(\frac{P_F}{\sqrt{8(N-2)}}\right)$. This threshold now determines the detection probability. We do not have a closed form equation for the detection probability. The results presented in Section V are obtained from simulation.

IV. Application to Modulation Classification

Here, we illustrate another application of our approach for classification of TCM signals vs. uncoded modulation signals. In particular we describe how the decision statistic in III-C can be applied to distinguish between 8-PSK TCM signals and uncoded 8-PSK signals. After down conversion and sampling the received signal, we obtain a sequence $\mathbf{r} = (\mathbf{r}_1, \mathbf{r}_2, \cdots, \mathbf{r}_n)$, where $\mathbf{r}_k = \mathbf{x}_n + \mathbf{v}_n$. Under the hypothesis $\mathcal{H}_1$ the sequence $\{\mathbf{x}_n\}$ is a coded sequence of symbols from 8-PSK TCM signal, and under the hypothesis $\mathcal{H}_2$, it is a sequence of independent 8-PSK symbols. $\{\mathbf{v}_n\}$ is an iid sequence of circularly symmetric Gaussian random variables.

The statistics of $T_3(\mathbf{r})$ under hypothesis $\mathcal{H}_1$ are the same as those in Section III-C. Under hypothesis $\mathcal{H}_2$ we have $E[T_3(\mathbf{r})|\mathcal{H}_2) = 0$. Moreover,

$$\begin{aligned}&\mathrm{var}[T_3(\mathbf{r})|\mathcal{H}_2] = \frac{1}{(N-2)^2}\times\\ &\sum_{k=2}^{N}E[\sin(2\theta_{n-2})\ \sin(4\theta_{n-1})\ \sin(2\theta_n))^2] \quad (15)\end{aligned}$$

Using the fact that under $\mathcal{H}_2$ consecutive symbols are independent and the symbols are uniformly distributed on a circle, after some mathematical manipulations, (15) can be simplified to get

$$\mathrm{var}[T_3(\mathbf{r})|\mathcal{H}_2] = \frac{1}{8(N-2)} \tag{16}$$

Therefore, P_F is given by (14).

V. Numerical Results

In this section we present our simulation results on the performance of the detector described in Section III-C. A TCM system with an 8-PSK modulation and the trellis of Fig. 2, [24], is used for transmission over AWGN channel. The received signal is down converted and sampled to obtain a data sequence of N samples. These samples are used to form the decision statistic in (9).

Fig. 4 shows the detection probability vs. SNR for a false alarm probability of $P_F = .1$ for three different values of N. If a detection probability of $P_D \geq 9$ is desired, [25], then for a given value of SNR, the required number of samples can be determined.

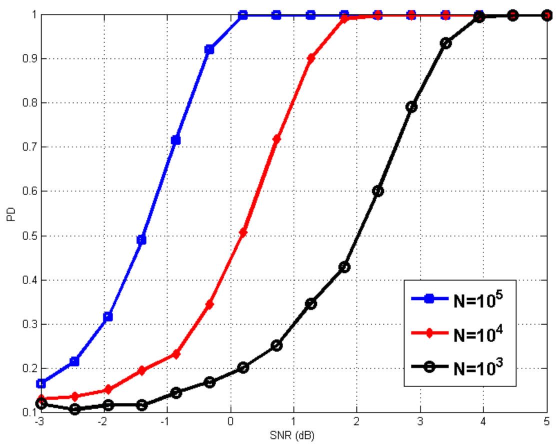

Fig. 4: Detection probability vs. SNR for $P_F = .1$.

Figs. 5 and 6 show the ROC curves for different sample size, N, at SNR=3 dB and SNR=5 dB, respectively. It can be seen that to obtain $P_F \leq .1$ and $P_D \geq .9$ a large number of samples required at SNR=3 dB that drops rapidly to a few hundreds as SNR increases to 5 dB. In Figs. 5 and 6 we also show the performance of an ideal energy detector (ED) which knows the level of noise power exactly. It is clear that the ideal energy detector outperforms the proposed detector even with a few data samples. However, it is well known that the energy detector requires knowledge of the noise power and when the noise power is estimated, the estimation error deteriorates the performance of this detector, a phenomenon known as "SNR wall", [26]. On the other hand the proposed detector is a CFAR detector and does not require knowledge of the noise power.

In Fig. 7 we show the error probability of the proposed classifier vs. SNR. It can be seen that for an SNR value of less than 13 dB, it achieves error probability of less than 1% with as few as 100 data samples.

VI. Conclusion

In this paper we derive the inter-dependency properties of symbols in a trellis coded modulation scheme. It is show that if the constraint length of the convolutional encoder is ν, then for TCM structures with good distance properties, $\nu + 1$ output symbols are dependent and no fewer than $\nu + 1$

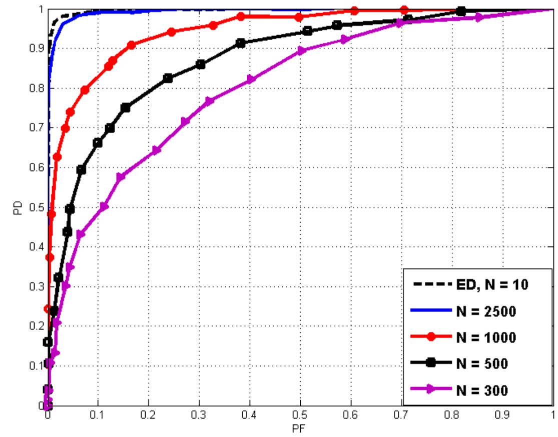

Fig. 5: ROC curve of the CFAR detector for SNR=3 dB.

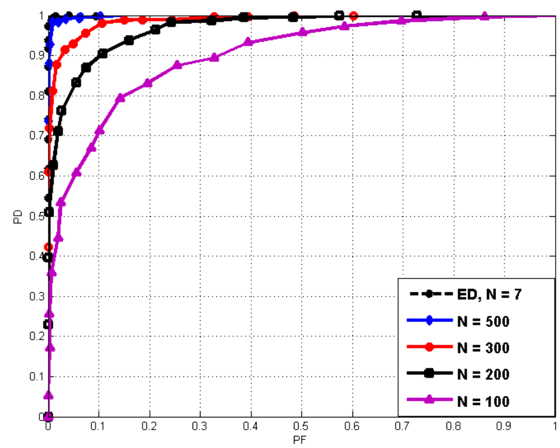

Fig. 6: ROC curve of the CFAR detector for SNR=5 dB.

symbols will be dependent. We develop decision statistics based on $\nu + 1$ consecutive symbols for detection of PSK modulated TCM signals in white Gaussian noise. Simulation results are provided for detection and false alarm probabilities. Application of our decision statistic for detection of a TCM structure vs. uncoded modulation is also discussed.

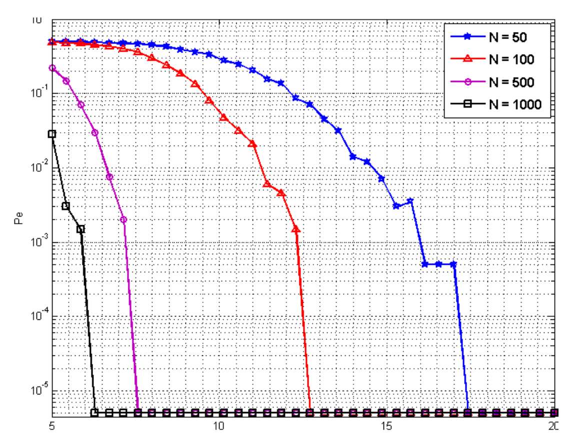

Fig. 7: Error probability of the proposed classifier vs. SNR.

REFERENCES

[1] E. D. N. 02-135, "Spectrum Policy Task Force Report," *Federal Communications Commission*, 2002.
[2] FCC-04-113, "Unlicenced operation in the tv broadcast bands; additional spectrum for unlicensed devices below 900 mhz and in the 3 ghz band," *Federal Communications Commission*, Nov. 2004.
[3] I. F. Akyildiz, W.-Y. Lee, M. C. Vuran, and S. Mohanty, "Next generation/dynamic spectrum access/cognitive radio wireless networks: A survey," *Computer Networks*, vol. 50, no. 13, pp. 2127–2159, 2006.
[4] M. Orooji, R. Soosahabi, and M. Naraghi-Pour, "Blind spectrum sensing using antenna arrays and path correlation," *IEEE Transactions on Vehicular Technology*, vol. 60, no. 8, pp. 3758–3767, Oct 2011.
[5] M. Orooji, E. Soltanmohammadi, and M. Naraghi-Pour, "Improving detection delay in cognitive radios using secondary-user receiver statistics," *IEEE Transactions on Vehicular Technology*, vol. 64, no. 9, pp. 4041–4055, Sept 2015.
[6] E. Soltanmohammadi, M. Orooji, and M. Naraghi-Pour, "Improving the sensing throughput tradeoff for cognitive radios in rayleigh fading channels," *IEEE Transactions on Vehicular Technology*, vol. 62, no. 5, pp. 2118–2130, Jun 2013.
[7] ——, "Spectrum sensing over mimo channels using generalized likelihood ratio tests," *IEEE Signal Processing Letters*, vol. 20, no. 5, pp. 439–442, May 2013.
[8] H. Urkowitz, "Energy detection of unknown deterministic signals," *Proc. IEEE*, vol. 55, no. 4, pp. 523–531, 1967.
[9] F. F. Digham, M. S. Alouini, and M. K. Simon, "On the energy detection of unknown signals over fading channels," *IEEE Trans. on Commun.*, vol. 55, no. 1, pp. 21–24, 2007.
[10] A. V. Dandawaté and G. B. Giannakis, "Statistical tests for presence of cyclostationarity," *IEEE Trans. Signal Process.*, vol. 42, no. 9, pp. 2355–2369, 1994.
[11] J. Lunden, S. Kassam, and V. Koivunen, "Robust nonparametric cyclic correlation-based spectrum sensing for cognitive radio," *Signal Processing, IEEE Transactions on*, vol. 58, no. 1, pp. 38–52, 2010.
[12] Y. Zeng and Y.-C. Liang, "Covariance based signal detections for cognitive radio," in *IEEE DySPAN*, Dublin, Ireland, 2007, pp. 202–207.
[13] S. Chaudhari, V. Koivunen, and H. Poor, "Autocorrelation-based decentralized sequential detection of ofdm signals in cognitive radios," *Signal Processing, IEEE Transactions on*, vol. 57, no. 7, pp. 2690 –2700, 2009.
[14] M. Naraghi-Pour and T. Ikuma, "Autocorrelation-based spectrum sensing for cognitive radios," *Vehicular Technology, IEEE Transactions on*, vol. 59, no. 2, pp. 718–733, 2010.
[15] T. Ikuma and M. Naraghi-Pour, "A comparison of three classes of spectrum sensing techniques," in *Global Telecommunications Conference, 2008. IEEE GLOBECOM 2008. IEEE*, 2008, pp. 1–5.
[16] M. Naraghi-Pour and T. Ikuma, "Diversity techniques for spectrum sensing in fading environments," in *Military Communications Conference, 2008. MILCOM 2008. IEEE*, 2008, pp. 1–7.
[17] G. Ungerboeck, "Trellis-coded modulation with redundant signal sets part i: Introduction," *Communications Magazine, IEEE*, vol. 25, no. 2, pp. 5–11, 1987.
[18] I. Bahceci and T. Duman, "Trellis-coded unitary space-time modulation," *Wireless Communications, IEEE Transactions on*, vol. 3, no. 6, pp. 2005–2012, 2004.
[19] W. Ruey-Yi and W. Yu-Lung, "On trellis coded noncoherent space-time modulation," *Wireless Communications, IEEE Transactions on*, vol. 6, no. 7, pp. 2432–2437, 2007.
[20] S. Ng, J. Chung, and L. Hanzo, "Turbo-detected unequal protection mpeg-4 wireless video telephony using multi-level coding, trellis coded modulation and space-time trellis coding," *Communications, IEE Proceedings-*, vol. 152, no. 6, pp. 1116–1124, 2005.
[21] M. Saito, S. Moriyama, and O. Yamada, "A digital modulation method for terrestrial digital tv broadcasting using trellis coded ofdm and its performance," in *Global Telecommunications Conference, 1992. Conference Record., GLOBECOM '92. Communication for Global Users., IEEE*, 1992, pp. 1694 –1698 vol.3.
[22] A. Aharony, C. Li, and M. Prokoptsov, "Octagonal quadrature amplitude modulation," mar 2015, uS Patent 8,995,573. [Online]. Available: https://www.google.com/patents/US8995573
[23] T. S. Rappaport, S. Sun, R. Mayzus, H. Zhao, Y. Azar, K. Wang, G. N. Wong, J. K. Schulz, M. Samimi, and F. Gutierrez, "Millimeter wave mobile communications for 5g cellular: It will work!" *IEEE access*, vol. 1, pp. 335–349, 2013.
[24] J. Proakis and M. Salehi, *Digital Communications*. New York: McGraw-Hill, 2008.
[25] IEEE, "Draft standard for wireless regional area networks," *IEEE P802.22TM/D0.4.8, Mar. 2008*, 2008.
[26] R. Tandra and A. Sahai, "SNR walls for signal detection," *IEEE J. Sel. Topics Signal Process.*, vol. 2, no. 1, pp. 4–17, 2008.